Hungarian University of Agriculture and Life Sciences

Doctoral School of Environmental Sciences

Integration of Remote Sensing and Field Data for Monitoring the Environmental Impact of Wetlands Restoration

Case Study: Al-Hammar Marshland, Southern Iraq

Ph.D. Thesis

Sadiq Al-Maliki

GÖDÖLLŐ, HUNGARY

2023

Hungarian University of Agriculture and Life Sciences, Hungary

Name of Doctoral School: Doctoral School of Environmental Sciences

Discipline: Environmental Sciences / Water Resources Management Engineering

Head of Doctoral School: Csákiné Dr Erika Michéli PhD
Professor, head of department
Department of Soil Science and Agrochemistry
Faculty of Agricultural and Environmental Sciences
Institute of Environmental Sciences

Supervisor(s): Professor Zoltán Vekerdy PhD, Department of Water Management and Climate Adaptation, Hungarian University of Agriculture and Life Sciences.

Professor Gusztáv Jakab PhD, Department of Water Management and Climate Adaptation, Hungarian University of Agriculture and Life Sciences.

Approval of Supervisor(s) Approval of Head of Doctoral School

Professor Zoltán Vekerdy PhD Professor Csákiné Erika Michéli PhD

…….

Professor Gusztáv Jakab PhD

……

Table of Contents

1 BACKGROUND

Worldwide diminishing water resources lead to environmental water scarcity, especially in the arid and semi-arid climatic areas. This leads to the need of efficient water management and monitoring methods.

Classifying marshlands in these regions and creating a land cover map is not a simple target. The dynamics of marshes is high, inundation and vegetation cover rapidly change due to the dynamics of the many drives affecting the marshlands, such as high evapotranspiration, temperature, and variation of inflow from rivers. In this study, we suggested a new approach for classifying the marshlands by a hierarchical classification of NDVI, NDMI, and NDWI. The results showed that the proposed method can efficiently classify marshlands. It can be used in other marshlands too, but the threshold for NDVI, NDMI, and MDWI have to be adjusted.

One of the major components of water balance (WB) in these zones is evapotranspiration (ET). ET estimation from wetlands (marshlands) in these areas plays a main role in water management. Information about it is needed for preserving marshlands, to take into account the imbalance between precipitation and potential evapotranspiration. For estimating ET, this study used Landsat images and the SEBS and SSEBop models for estimate ET_a, and ET_a products from MODIS (MOD16) and FAO's WaPOR system. These actual evapotranspiration from models and products were compared to ET_0 defined by the Penman-Monteith method using metrological data measured at a meteorological station nearby the test area by assumed that in these wetlands, ET_0 and ET_p are equal. Since there is always water and no water stress is present, we can assume ET_a is equal ET_p maybe it is a little lower but not higher (i.e., no water stress is present).

This study focuses on (1) classifying and analysing the wetlands, (2) finding the best ET monitoring method by integrating the data from metrological and remote sensing to calculate actual ET with spatial distribution instead of using calculated ET from metrological data only, (3) then use the in situ data together with the classification results to analyse scenarios for water routing/management **Figure 1**.

In this study, the test area was the Al-Hammar marsh in the southern part of Iraq. This marsh was exposed to draining measures in the nineties. It also strongly depends on upstream water management activities in its catchment, inside and outside Iraq. Many of these measures focused on controlling and altering natural hydrology for the retention of water. The west part of Al-Hammar marsh was supplied with the effluent agricultural brackish water of the Main Outfall Drain (MOD), in order to address the water shortage problem and avoid complete drying up. Resultingly, salts started to accumulate in the marsh.

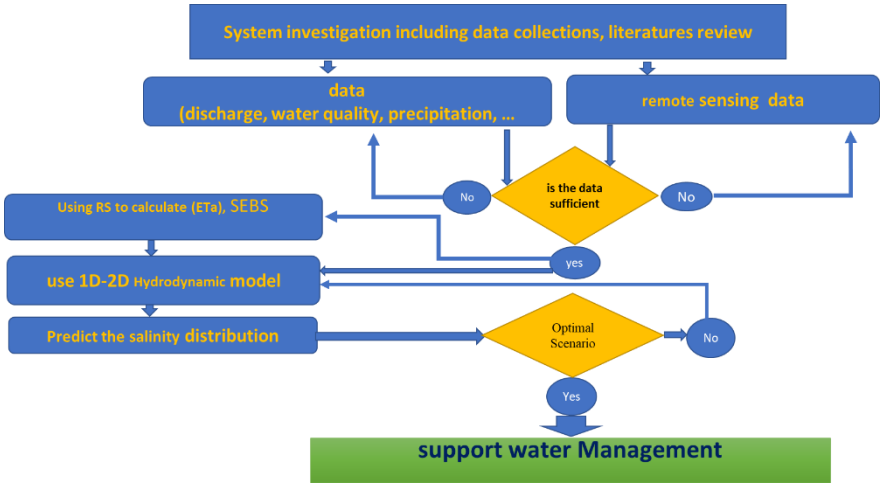

Figure 1. The research processes.

1.1 Research objective

The main research objective is to develop a remote sensing method based on data integration for analyses, classification, and monitoring of the environmental impact of wetlands restoration.

The test area of the research is the Mesopotamian marshlands (west part of Al-Hammar marsh).

1.2 Sub Objectives

1. Develop a fast wetland classification and monitoring method based on remote sensing data.
2. For evaluating and testing water balance scenarios under different operational conditions, calculate the time series of actual evapotranspiration from satellite images using different surface energy balance models, then compare them with the evapotranspiration calculated from metrological stations to find the optimal data processing method.
3. Analyse different water balance scenarios under various operational conditions based on field discharge measurements, collected water samples, and water losses by ET calculated from RS data.

2 MONITORING AND CLASSIFICATION OF WETLANDS

The land cover for wetlands in arid and semi-arid regions is very dynamic due to extreme driving factors, like high temperature, vapour deficit in the air, extreme rainfall events, and floods on feeding rivers, which led to rapid and dramatic changes in the water and vegetation cover in wetlands. The supervised and unsupervised methods cannot be applied because these methods need detailed information and many training data.

To understand these systems and support their management, a simple, robust, and fast classification and monitoring method is required with adjustment of the threshold, which can be done with very little field data.

Remotely sensed data are optimal to cover the large spatial extent of the wetlands and overcome issues related to the limited access to certain regions. This chapter suggests a new approach for classifying marshlands and monitoring land cover changes in them. The analysis is based on a hierarchical classification of optical indices: the Normalized Difference Water Index (NDWI) (McFeeters, 1996), the Normalised Difference Moisture Index (NDMI) (Gao, 1996), and the Normalised Difference Vegetation Index (NDVI) (Tucker, 1979). Compared to the UNEP methodology (UNDP, 2010), the proposed approach results in three extra classes: wet soil, dry soil, and open water.

2.1 Approach Description

Characterisation of wetlands in the optical part of the electromagnetic spectrum is typically achieved by analysing the key land cover units' spectral characteristics based on their visible and infrared reflectance. The separation

of open water, vegetation, and soils is best achieved using the red (0.60–0.69 μm) and near-infrared (0.70–1.30 μm) wavelength ranges (Siegmund and Menz, 2005). Water shows relatively low or no reflectance in near-infrared and maximum reflectance in the blue wavelength range. Chlorophyll in healthy vegetation is a good absorber of electromagnetic energy in the visible spectrum, especially in red, and strongly reflects in the near-infrared.

The different vegetation types show well-detectable differences in these characteristics. Bare soil has a gradually increasing reflectance from the visible range through the near infrared to the middle infrared, depending on soil characteristics (texture, moisture content, and organic content). Historically, a combination of analogue panchromatic and infrared photography has been used for such analysis, although now digital multiband scanners have become the preferred medium (Verhoeven, 2008). A wide range of aerial and space-borne satellite imaging systems provide data over this spectral range but differ substantially in their temporal imaging frequency (overpasses per year), swath diameter, spatial resolution, and cost. The selection of imaging systems is enforced by a trade-off between these variables and must be attuned to the study's objectives, not vice versa.

In 2010, UNEP, UNDP, and CRIM suggested a method based on NDVI to classify marshlands, and thresholds have been developed to describe the status of marsh vegetation. The UNEP study (UNDP, 2010) showed that NDVI values greater than 0.125 represented vegetation cover. Sparse vegetation was found to correspond to NDVI values between 0.125 and 0.25, while medium-density vegetation was associated with NDVI values between 0.25 and 0.5. Dense vegetation was found to occur in areas with NDVI values above 0.5. Unfortunately, areas with NDVI values between 0.125 and 0.25 (sparse

marshland vegetation) showed large commission errors, falsely expanding marshland areas. The errors resulted mainly from the inability of the NDVI to differentiate between submerged sparse water vegetation and sparse terrestrial vegetation.

Consequently, there was a need to initially delineate the marshland areas as a function of their wetness before classifying the vegetative cover status in **Figure 2**. Thresholding of NDMI was used to delineate areas with high levels of soil moisture (Hunt and Rock, 1989). NDMI values greater than zero were identified as wet regions (Rokni *et al.*, 2014). Regions covered with open water were identified by their MNDWI values: regions with an MNDWI value greater than zero were defined as open water (Xu *et al.*, 2006; Ji, Zhang and Wylie, 2009; Fisher, Flood and Danaher, 2016).

2.2 Indices calculation

Three spectral-based indices were generated and used to assess the temporal variability in the inundation area of the marshes as well as the health of the vegetation coverage. The formulas of the indices used in this study are listed in **Table 1**.

Table 1: Spectral indices used to assess the Iraqi marshlands.

Index	Equation	
NDVI	$NDVI = \frac{(NIR-R)}{(NIR+R)}$	(Tucker, 1979)
NDMI	$NDMI = \frac{(NIR-SWIR_1)}{(NIR+SWIR_1)}$	(Gao, 1996)
MNDWI	$MNDWI = \frac{(Green-SWIR_1)}{(Green+SWIR_1)}$	(Xu, 2006)

NIR: Near-infrared (Band 4 in Landsat 5 and 7; Band 5 in Landsat 8); R: Red (Band 3 in Landsat 5 and 7; Band 4 in Landsat 8); B: Blue (Band 1 in Landsat 5 and 7; Band 2 in Landsat 8); $SWIR_1$: Shortwave infrared (Band 5 in Landsat 5 and 7; Band 6 in Landsat 8); Green: (Band 2 in Landsat 5 and 7; Band 3 in Landsat 8).

The spatial extent of the marshlands over time was assessed based on the methodology presented in **Figure 2**. This region was defined as the spatial extent of the marsh in each satellite image.

This methodology checked every pixel in the study area. The open-water regions were identified as pixels with NDWI values greater than zero. Non-water but wetted cells were then divided into vegetated areas and wet soils. If the NDWI value is less than zero, then other indices are checked. If NDWI < zero, then the wetted regions in the marsh are identified by excluding all areas with an NDMI < zero, considering it as a dry area or no marsh. However, if NDMI > 0, then it is considered vegetated area or wet but non-vegetated area (wetted soils) in marshlands and compared with NDVI indices.

Vegetated areas were selected as wet regions (NDMI >0) and NDVI > 0.125. Vegetated areas were further classified into densely vegetated (NDVI>0.5), medium- (0.25<NDVI<0.5) and low-density vegetation (0.125<NDVI<0.25) based on the UNEP-defined NDVI thresholds (UNDP, 2010), A model in ArcGIS 9.2[1] is used to present this methodology to develop the condition of raster for every single pixel.

[1] ArcGIS 9.2 version is sufficient for this study.

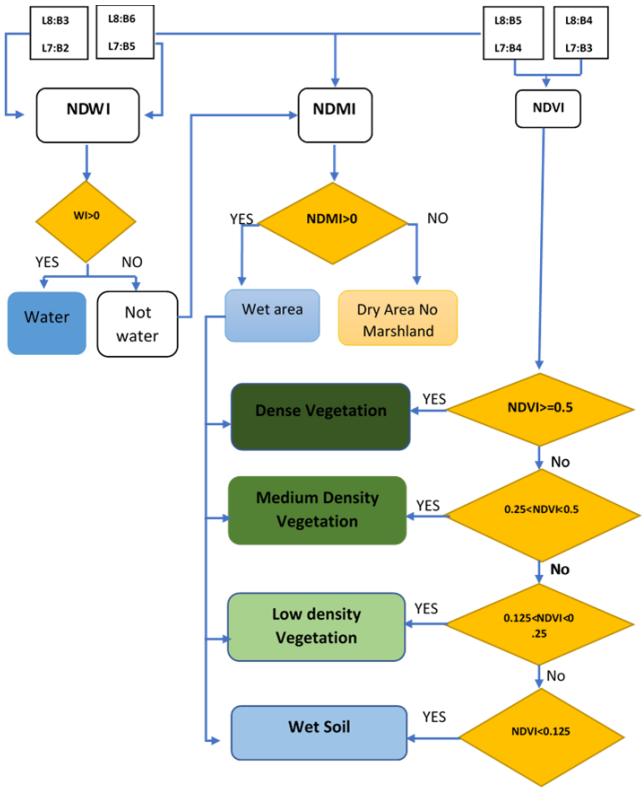

Figure 2. Method for identifying marshland extents, open waters, and vegetated areas.

2.2 Results and Discussion

Based on the methodology, the spatial extent of the marshlands was assessed in each satellite image. A visual inspection reveals the extraordinary degree of spatial changes in its extent and vegetation cover during the study period. After a strong presence of vegetation in 1991, the 2002 image shows a near-complete lack of vegetation in the Al-Hammar marsh, while there is again vegetation cover in 2017.

The marsh lost a large portion of its vegetation cover in the year 2002 as a result of drainage and desiccation activities carried out by the Iraqi regime during that period. **Figure 3** show the spatial distribution for the six classes for 1991, 2002, and 2017, respectively. The area covered with water dropped

from more than 800 km^2 in 1991 to less than 20 km^2 in 2002. Fortunately, recent restoration efforts reversed some of these losses. In the past four years (2015-2018), the vegetated area has been above the 500 km^2 mark 75% of the time, as shown in **Figure 3**. A close observation of the vegetation density across three years, namely, 1991, 2002, and 2017, indicates the dramatic degradation that the Al-Hammar experienced in 2002 **Figure 3** The marshland lost all vegetation.

The impact of the marsh restoration appears from 2015 until 2018. However, at the marshland level, the 2018 vegetation coverage and water are still lower than that of 1991 **Figure 3**. Vegetation and water between April and September covered between 1150 and 1430 km^2 of the marshland in 1991; levels in 2018 have not managed to grow beyond 1150 km^2 for water and vegetated area.

Moreover, the composition of the vegetation changed, whereby the levels of high and medium-density vegetation dropped compared with the sparsely vegetated. Between April and September, vegetation covered 400 and 570 km^2 in 1991, less than 50 km^2 in 2002, and 170–490 km^2 in 2018. Moreover, the vegetation composition experienced a change, whereby the levels of high- and medium-density vegetation dropped compared to the sparsely vegetated area. The proposed approach can monitor the changes regarding water and land cover with time for the marshlands.

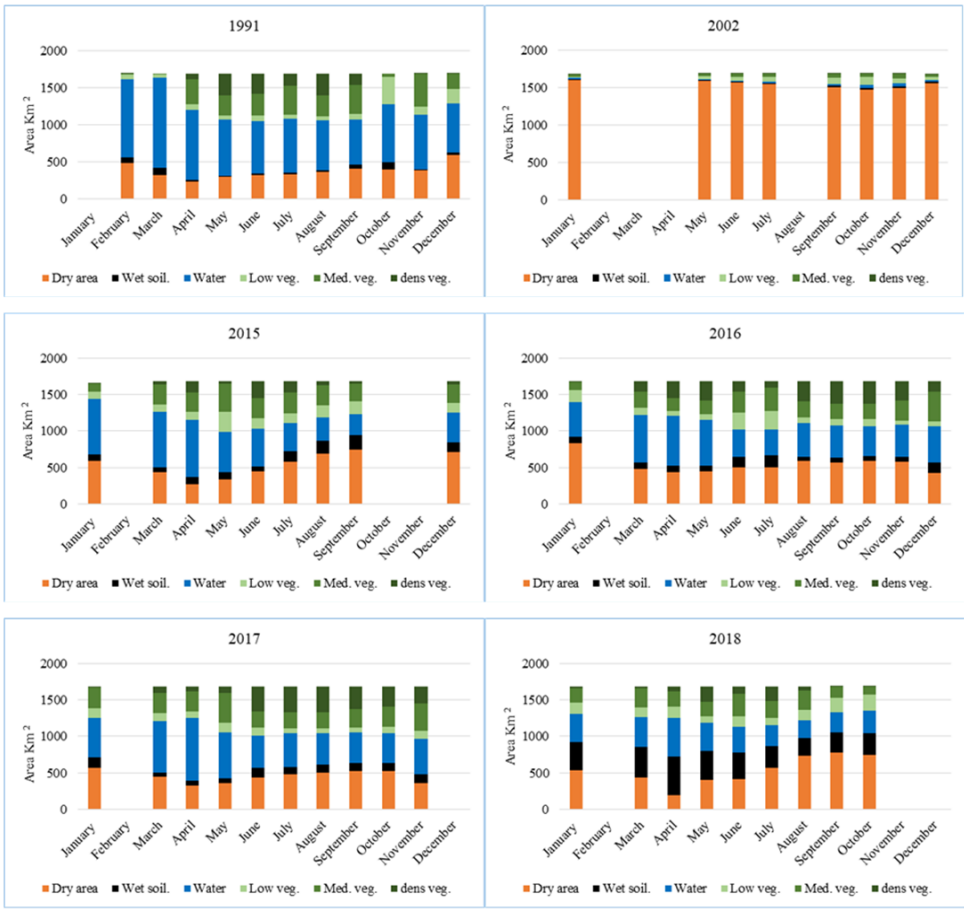

Figure 3. Monthly changes in vegetation type and water cover areas in the Al-Hammar marshland: comparison between 1991, 2002, 2015, 2016, 2017, and 2018.

In the past four years (2015–2018), the vegetated area has been above the 500 km^2 mark 75% of the time. Open water in 2017 is higher than in 1991 because the marsh area was reduced from 4500 km^2 in 1991 to 1600 km^2 after 2003. Generally, the open water areas were higher during the winter months than the summer months because of high evapotranspiration.

2.3 Sensitivity to Spatial Resolution

To analyse the effects of different spatial resolutions, two images from different sensors (Sentinel-2 with 10 m resolution and Landsat 8 with 30 m resolution) taken on the same day (24 August 2017) were compared. We analysed the western part of the study area, where the two images overlapped, and used the same method to classify the marshland. The results are shown in **Figure 4**.

The two resulting maps, resampled to 10 m spatial resolution, were compared in a confusion (error) matrix. There is 78% overall agreement between the two classified images, which can be considered a good match. The complex patchy pattern of the wetland results in relatively more mixed pixels in the Landsat image, with the coarser resolution, than in the Sentinel image, leading to more mismatch of spectrally different classes (e.g., water vs. dry soil).

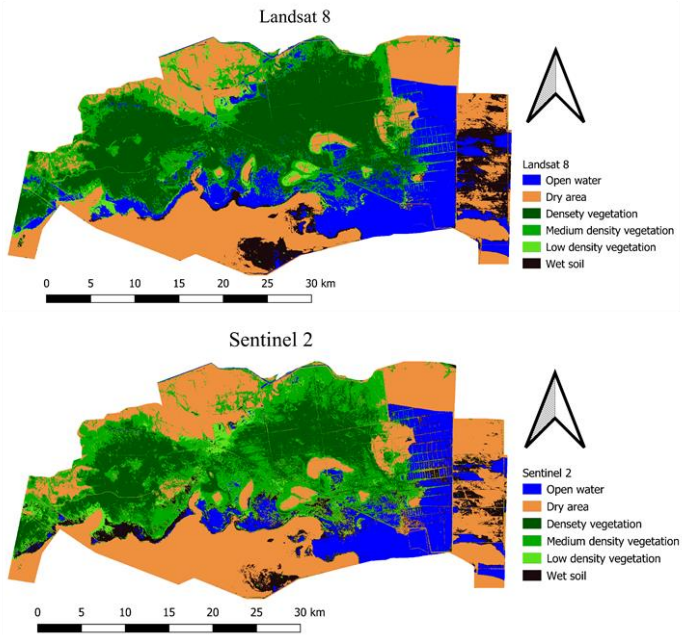

Figure 4. A comparison between the classification results for part of the study area according to the proposed approach for two types of satellite images, Landsat (a) and Sentinel 2 (b), for the same day. A significant similarity between the two images is found, and this finding confirms that the proposed approach works effectively on different satellite images.

3 ESTIMATING EVAPOTRANSPIRATION IN THE MARSHLANDS

This chapter presents the most common and efficient methods to calculate the actual evapotranspiration time series from satellite images and compares the results with the evapotranspiration values calculated from data of metrological stations and how integrated the data from metrological and remote sensing to calculate ET with spatial distribution instate of using calculated ET from metrological data only (Musa *et al.*, 2015). Therefore using a hydrodynamic model for more efficient water management for wetlands and open water bodies (Domeneghetti 2014).

To find an optimal model or product to estimate ET_a in marshlands, two RS data-based models (SEBS and SSEBop) using Landsat 8 images from 2016 and 2017 were chosen and compared with two ET_a products (MODIS MOD16 and FAO's WaPOR ET).

3.1 EO-based ET quantification models

3.1.1 Surface Energy Balance System (SEBS)

Su (2002) introduced this single-source model for calculating turbulent energy fluxes based on the surface energy balance equation. The SEBS model designed to estimate ET_a needs two types of data: the first group includes land surface albedo, emissivity, temperature, fractional vegetation coverage, and the height of vegetation (related to roughness height). These data can be retrieved from satellite images. The second group comprises air pressure, temperature, humidity, wind speed at a reference height, downward solar radiation, and downward longwave radiation. These parameters can be determined directly from meteorological data or by a model. Situ measurements are validated to observe ET with 10%–15% uncertainty (Su et

al., 2005), and others show that the uncertainty is within the range of 30% (Liou and Kar, 2014).

3.1.2 SSEBop model

Senay et al. (2007) simplified the surface energy balance equations (SEB) based on the basic assumptions of SEBAL and METRIC to estimate ET as a linear function of surface temperature. Unlike the original SEB methods, the SSEBop model does not solve for the energy balance term *H* explicitly. According to Senay et al. (2013) and on the basis of radiation balance principles for clear sky: 'dry /hot' temperature (*Th*) is used for no or limiting conditions of latent heat flux. 'Wet/ cold' temperature (*Tc*) is used for no or limiting conditions of sensible heat flux for each pixel. Senay defines differential temperature (*dT*) between two limiting conditions.

3.1.3 FAO's WaPOR ET product

To improve water use efficiency, the Food and Agriculture Organisation of the United Nations (FAO) developed the WaPOR methodology and maintains the WaPOR database (FAO, 2020) at different scales. It provides open-access monthly actual ET and interception (ETIa), which can be found at https://wapor.apps.fao.org/home/WAPOR_2/2. ETIa is based on the two-source model (ETLook) described by (Bastiaanssen 2012). It uses Penman–Monteith equations (Allen 1998b) with RS data, such as solar radiation, surface albedo, NDVI, land cover, soil moisture and uses measured meteorological data (air temperature, solar radiation, wind speed and vapour pressure) for the calculation of soil evaporation, vegetation transpiration and interception.

The monthly available ETa products for 2016 and 2017 were downloaded from the database with 100 m spatial resolution for the study area.

3.1.4 MODIS ET data (MOD16)

MOD16 is an ET_a product based on an algorithm that uses the Moderate Resolution Imaging Spectroradiometer (MODIS) sensor data, meteorological data from the Global Modelling and Assimilation Office, and a satellite-based soil moisture product. MOD16 values represent the sum of evaporation from canopy stomata, interception and bare soil. The algorithm is based on the modified Penman–Monteith equation and uses the estimated canopy surface, aerodynamic conductance terms and soil moisture defined by a set of semiempirical equations developed by Mu, Zhao and Running (2011) for different land cover types. These equations require calibration for ET_a measurements with situ ET_a, such as eddy flux towers, and depend on the accuracy of the land cover type. However, uncertainty in some ET estimates from different models can range from 10% to 30%, and maximum absolute errors are 24% of the ET measurements (Mu, Zhao and Running, 2011).

Monthly ETa MOD16 data were downloaded with 1000 m spatial resolution for 2016 and 2017 and clipped for the study area from https://lpdaac.usgs.gov/.

3.2 Metrological Ground Station Data

The following daily data were used from the Al Chibaeich Metrological station, located at E: 47.07, N: 30.94 in the marsh. The maximum and average wind speed, maximum and minimum temperature, and relative humidity. Furthermore, the sum of solar radiation, rainfall and sunshine hours were collected from the An Nassiriyah station, located at E: 46.14, N: 31.05. The data sets cover the period from 2015, 2016, and 2017.

3.3 Analysis of the ET Quantification Models and Products Results

The following subsections describe the ET_a quantification results of the Al-Hammar marsh.

3.3.1 SEBS Model: Temporal and Spatial Variation of ET

Used Integrated Land and Water Information System (ILWIS) software from the International Institute for Geo-Information Science and Earth Observation (ITC) University of Twente Netherlands (www.itc.nl/ilwis/download/ilwis33) for calculating the spatial ET_a for all images in. **Table 2** shows the Monthly ET_a estimates from SEBS during 2016, and 2017. The results, as expected, showed spatial distribution of ET_a values variations over the study area and higher ET_a in the summer than in winter. The maximum daily ET_a values are located where the dense vegetation is in the centre of the study area during summer, but during winter, ET_a is higher when the area consists of a mixture of open water and low vegetation cover. For 2016, the ET_a was 9.83 mm day $^{-1}$ for July and 2.74 for December, and for 2017 the ET_a was 9.93 mm day $^{-1}$ for July and 3.53 mm day $^{-1}$ for December. The minimum ET_a during the study time was 0 mm day $^{-1}$ and located where the soil is very dry in agricultural areas in the north or inside the marsh when the houses. SEBS worked well in the areas with different land cover types, i.e., open water, vegetation, bare soil, and wet soil, and there is no missing data of ET_a in any pixel. The ET_a close to Al Chibaeich metrological station ranged between 1.01 and 9.98 mm day^{-1} during the three years, with a maximum ET_a on July 18, 2015.

3.3.2 SSEBop Model: Temporal and Spatial Variation of ET

The Python code belonging to the Iraq Ministry of Water Resources (Baghdad, Iraq) and data from the Global Data Assimilation System (GDAS) were used to calculate the spatial distribution of ET_a from 19 satellite images in 2016 and

2017 for comparison with the SEBS model. **Table 2** shows the variation of ET_a defined by the SSEBop model in the study area during this period. There is convergence in the values for the months corresponding to the length of the years of study; there is some distinction in ET_a over 2016 and 2017.

Separating the evaporation of the open water from the ET in the area covered with vegetation was difficult in the SSEBop model results. For 2016, the maximum in July was 11.6 mm day $^{-1}$ and in January 2.1 mm day $^{-1}$; for 2017, the ET_a was 11.3 mm day $^{-1}$ for July and 2.74 for December. The minimum ET_a during the study time was 0 mm day $^{-1}$ and located where the soil is very dry in the agriculture area in the north or inside the marsh where the villages are located. Thus, the SSEBop was used to calculate short grass reference ET_0 in the global data product by GDAS, and the scaling coefficient *K* in Equation 8 needed to be adjusted by using ET_0 from the local metrological station. GDAS is a gridded product available every 6 hours (Senay 2008). The ET_a close to Al Chibaeich metrological station during the two years ranged from 0.75–8.75 mm day^{-1}, and the maximum ET_a was 11.6 mm day^{-1} on July 4 2016.

3.3.3 FAO's WaPOR product: Temporal and Spatial Variation of ET

The WaPOR ETI_a product showed spatial and temporal variations. **Table 2** shows the monthly ETI_a during 2016 and 2017.

The product showed spatial distribution of ET_a values varies over the study area and showed higher ET_a in the summer than in winter. Generally, during the summer, the maximum daily ET_a values are located when the dense vegetation is in the centre of the study. In the winter maximum, ETa from the area is mixed between open water and low vegetation cover. In 2016 the

maximum ETa in June was 10.8 mm day $^{-1}$, and the minimum in December was 2.5 mm day $^{-1}$; in 2017, the maximum ETa was 11.5 mm day $^{-1}$ for July, and the minimum was 2.7 mm day $^{-1}$ in January. The product record minimum ETa is 0 mm day $^{-1}$ during 2016 and 2017 in different areas, especially in the south when the wet and dry soil is mixed.

3.3.4 MOD16 product: Temporal and Spatial Variation of ET

The product showed spatial distribution of ET_a values varies over the study area and showed higher ET_a in the summer than in winter. The maximum daily ET_a values are located at the dense vegetation in the center of the study area during summer and winter. For 2016, the maximum in July was 13 mm day $^{-1}$ and the minimum was in January, 2 mm day $^{-1}$; for 2017, the ET_a was 13 mm day $^{-1}$ for July and 2.7 mm day^{-1} in January. The minimum ET_a during the study time was 0 mm day $^{-1}$ and was located in different areas, especially in the south at pixels areas were mixed between the wet and dry soil.

The monthly ET_a close to Al Chibaeich metrological station changed during the two years from 0.64 to 8.29 mm day^{-1}, and the maximum ET_a was reached in June 2017.

The scheme shows a maximum of 13 mm day $^{-1}$, but this is energetically impossible; therefore, MOD16 in the wetlands needs to be calibrated by multiplying it with a bias fixing factor (Leonce, 2021).

Table 2: Monthly ET_a estimates from SEBS, SSEBop, MOD16, WaPOR, and calculated ET_0 at the Al Chibaeich metrological station for the years 2016 and 2017.

Date	SEBS ETa	SSEBop ETa	Mod16 product ETa	FAO product ETa	ETo
1/10/2016	1.21	0.75	0.64	0.43	2.1
3/30/2016	4.14	3.06	2.2	1.23	5.4
4/15/2016	6.06	3.19	3.46	2.27	5.6
5/17/2016	7.12	5.8	6.51	3.53	6.9
6/18/2016	7.52	8.1	7.52	3.77	6.4
7/4/2016	7.74	8.75	7.97	3.71	8.1
8/5/2016	7.35	6.01	5.9	3.67	6.8
9/22/2016	5.53		4.32	3.37	6.6
10/8/2016	4.21	3.02	2.46	2.48	4.7
11/9/2016	2.5	1.73	1.74	1.55	3.0
12/11/2016	1.01		0.98	0.67	2.1
1/12/2017	1.38	1.29	1.37	0.62	2.8
3/17/2017	4.08	4.05	3.39	1.54	4.5
4/2/2017	5.89	4.47	7.13	3.1	5.4
5/20/2017	7.96	8.16	7.13		8.3
6/21/2017	5.54	8.28	8.29	4.49	8.9
7/23/2017	7.4	6.62	8.09	4.31	7.2
8/8/2017	6.9	5.94	5.74	4.01	6.9
9/9/2017	5.82	4.36	3.35	3.44	6.0
10/11/2017	4.14	1.92	2.43	2.49	5.1
11/28/2017	2.23	1.26	1.42	1.43	1.6

3.4 Validation and Comparison of the Results

Since no in situ ET_a measurements were available in this area, the validation was carried out using the ET_0 calculated from the meteorological station at Al Chibaeich, representing the "ground truth". We compared the different ET_a maps as follows: 50 maps were calculated by SEBS, 19 calculated by SSEBop, 23 maps from MODIS ET_a products downloaded from the database, and 19 ET_a maps from the WaPOR products database were downloaded.

The ET_0 values calculated from the station should be multiplied with the coefficient K_c to calculate the ET_p, as shown in **Equation 1**. According to Allen (1998b), the K_c values for reed swamp with standing water are 1.0, 1.2, and 1.0 for K_{c_ini}, K_{c_mid}, and K_{c_end}, respectively, and for reed swamp with moist soil, the same values are 0.9, 1.2 and 0.7. The different phenological phases are usually present simultaneously in the vegetation cover of the study area. Therefore, it is assumed that in these wetlands, ET_0 and ET_p are equal.

Since there is always water and no water stress is present, we can assume ET_a is equal ET_p maybe it is a little lower but not higher (i.e., no water stress is present).

$$ET_p = ET_0 \times K_c \quad (1)$$

Where: ET_p is the potential ET for the crop, K_c is the crop coefficient for the particular crop.

The ET_0 calculator software of FAO (version 3.2) was used for calculating the daily reference evapotranspiration for the analysed two years for validation.

The comparison of calculated ET_0 with estimated ET_a from the different methods gives confidence in the generic applicability of each analysed method for ET_a estimate, since the methods effectively tracked the temporal variation of the ET_0 defined from the meteorological data **Figure 5**.

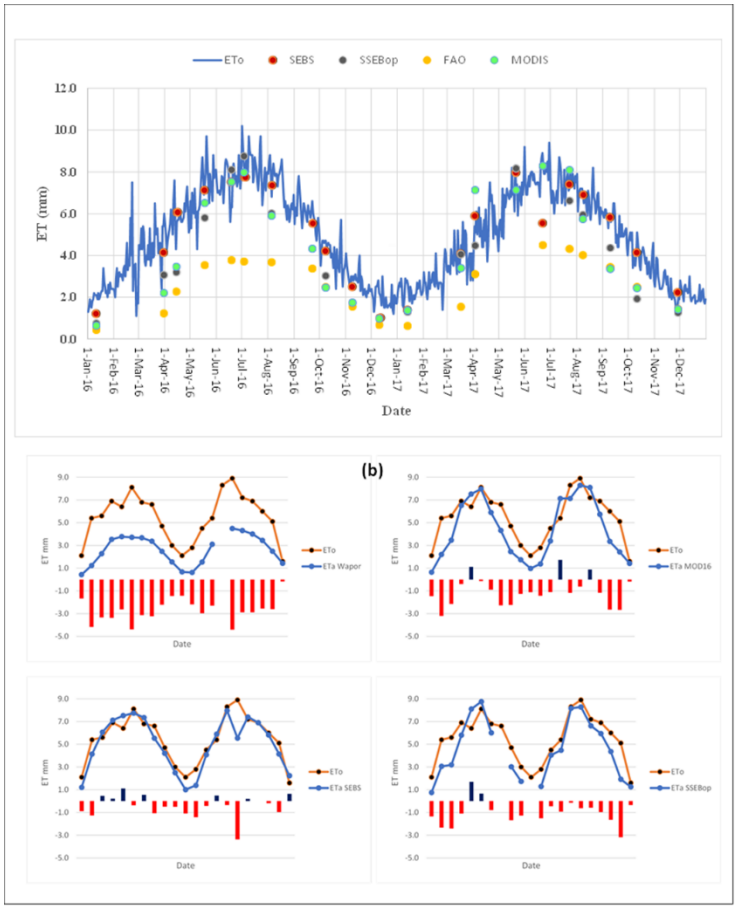

Figure 5. (a) Daily ET_0 and temporal ET_a variation satellite overpasses based on the models and products close to Al Chibaeich metrological station changed during the two years 2016 and 2017. (b) Residual of calculated ET_0 and estimated ET_a of models and products for same dates and compared with ET_0.

4 WATER BUDGET

This chapter discusses the flows within the marsh. It is based on data obtained by in situ flow measurements, sampling, and measuring TDS on the inflow drains in the marsh. These data are combined for tracking the water movement within the wetland (hydrological routing); ET calculations from the satellite images in chapter five and the data measured in additional to the data available from MoWR and the Ministry of Environment (MoE) used in this chapter and all data are monthly.

4.1 Evapotranspiration in the Marshlands

The region of the Al-Hammar marsh has high evapotranspiration ET_a with extreme cases of drought. **Figure 6** shows the ET_a calculated from meteorological data. The mean annual ET_a is 3011 mm (UNEP, 2006). In the present study, based on the SEBS model for the 2015–2017 period, The mean annual evapotranspiration was 2464 mm **Figure 7.** It is noticeable that there is a difference between the distribution of monthly ET_a between the UNDP study and the present study because UNDP used the data from metrological stations, which are far more than 100 km from the study area.

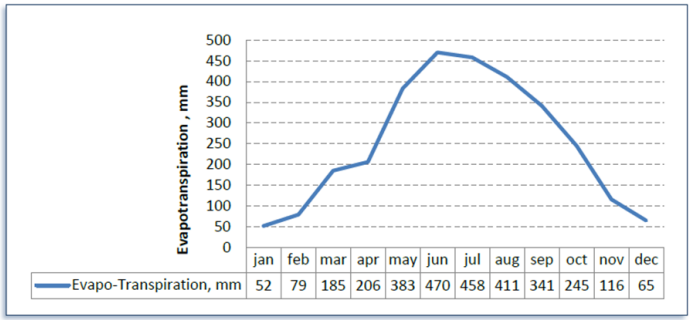

Figure 6. Monthly mean evapotranspiration within Al-Hammar marsh (CRIMW, 2007).

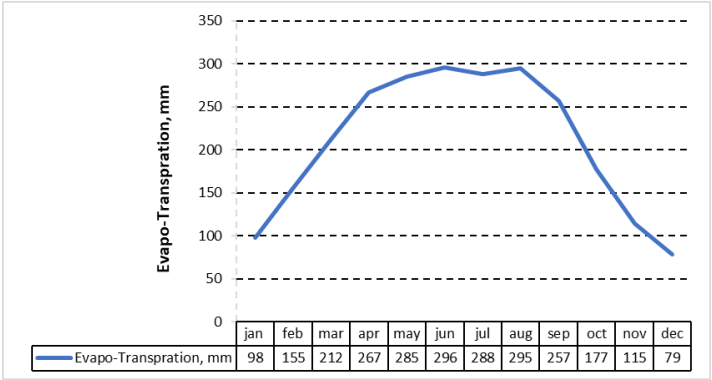

Figure 7. Monthly mean actual evapotranspiration in the Al-Hammar marsh based on the method defined in Chapter 5, using the data from 2015 till 2017.

4.2 Fieldwork

Field campaigns were carried out for collecting complementary data that are essential for this study, to understand the nature and features of the study area, and check the accuracy and reliability of the recorded data. A complete set of monthly discharge measurements for the main feeders of the marsh was carried out during 2015–2017 in cooperation with CRIMW, and water samples to define the TDS concentration were also collected.

4.2.1 Water Quantity

Monthly discharge measurements of the main feeders of the west part of the Al-Hammar marsh were carried out with cooperation of CRIMW during 2015-2017. An Acoustic Doppler Current Profiler (ADCP) was used for the discharge measurement. **Figure 8** shows the monthly discharge data from 2015 till 2017. The total average monthly discharge supplied to the marsh between 2015–2017 by all feeders were 32.3 m^3/s (16.7 from Euphrates feeders, and 15.6 m^3/s from the Al Khamissiya); thus, the average discharge from the Euphrates River feeders was about 52% of the total inflow to the marsh.

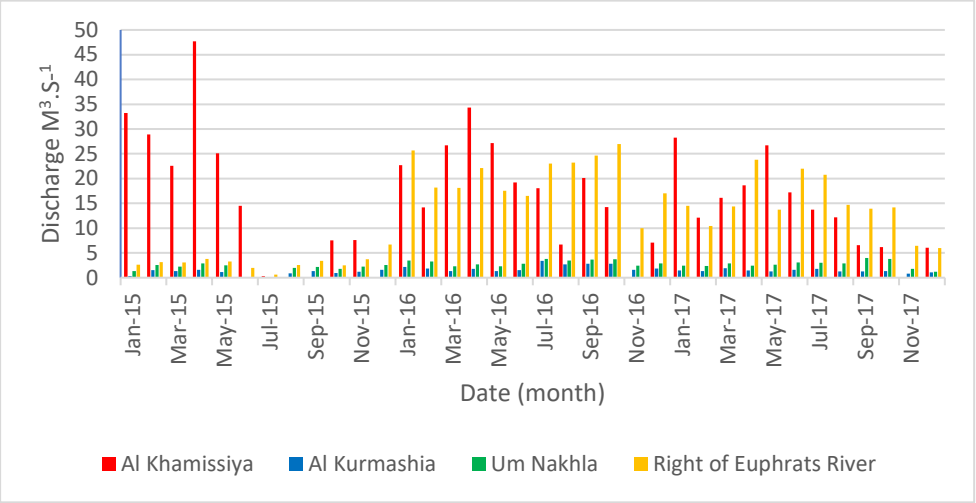

Figure 8. Monthly discharge to the Al-Hammar marsh through the feeders in $m^3 s^{-1}$ from 2015 to 2017 (Source of data: Ministry of Water Resources, Iraq). (Al-Maliki, 2018)

4.2.2 Water Quality

For this study, it was decided with MoE and WoWR to add locations also inside the marsh for sampling, using YSI Water Quality Sampling and Monitoring Meters. The monthly data is available for all locations from 2015 till 2017. The measurement results are shown in **Figure 9**. The water samples were collected from a depth of 20 cm. The TDS concentration of the collected samples was measured using the YSI 650 MDS instrument.

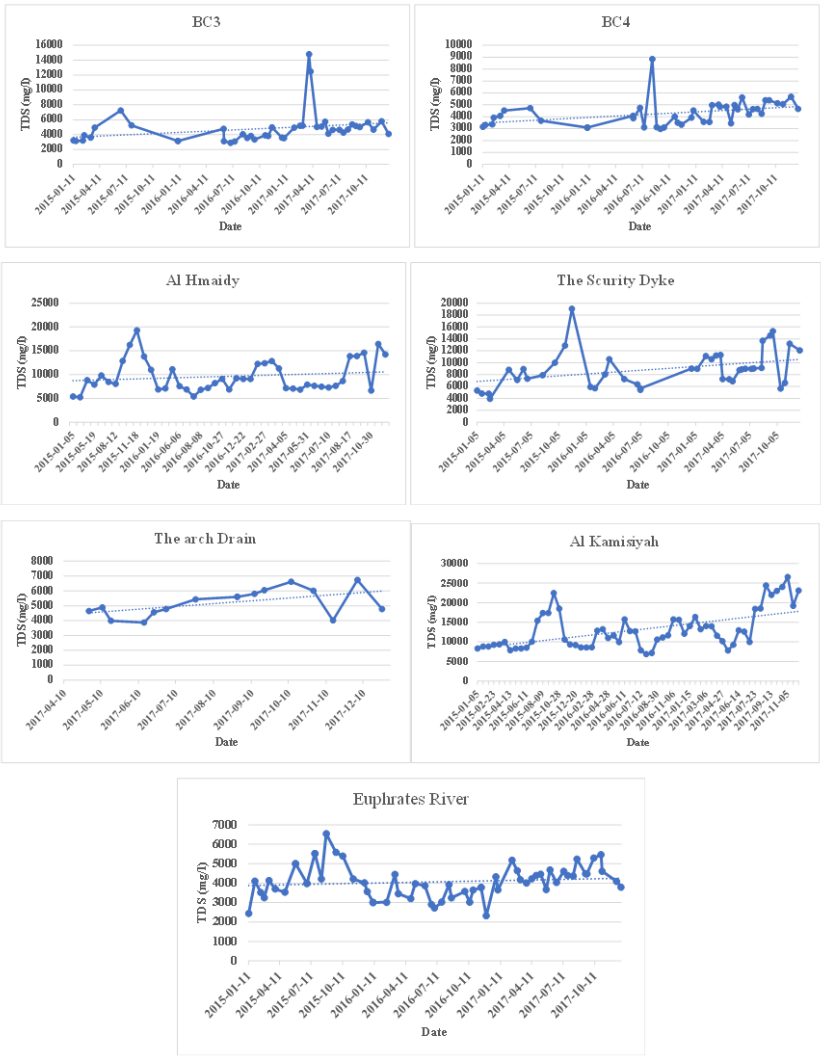

Figure 9. TDS of the Euphrates River, MOD upstream of the Al-Hammar marsh, and the sampling points inside the marsh from 2015 to 2017 (with cooperation of Ministry of Environmental, Iraq).

4.3 Water budget calculation

The field measurement showed that the TDS concentration of the feeders from the Euphrates River ranged between 2320 and 6540 mg/l with an average of 2067 mg/l. The TDS concentration of the Al Khamissiya Canal was ranging between 6900 mg/l and 26522 mg/l with an average of 13130 mg/l during the

period above, so the TDS of the Al Khamissiya Canal was more than four times higher than the TDS concentration in the Euphrates River **Figure 9**.

By applying the basic principle of mass conservation, the hydrological routing of the west part of the Al-Hammar marsh was carried out. The required inflow to maintain a constant marsh area equals the evaporation from this area, plus an outflow required for flushing out some of the salts accumulated within the marsh.

Maintaining a constant area can help in flushing out the salts accumulated within the marsh when there is a surplus inflow. Moreover, maintaining a constant area helps fix the marsh's boundaries for future planning of projects. The constraints for maintaining a constant area are the sum of outflow from the marsh, including evapotranspiration subtracted the rainfall from it and the outflow to flush out the accumulated salts within the marsh, and the sum of inflow to the marsh, including the inflow of the feeders from the Euphrates River and the water of the MOD supplied by Al Khamissiya Canal.

Discussion with the experts of MoWR and the strategical study for water and land in Iraq for 2015-2035 (MoWR, 2014) show that the discharge of the feeders to the marsh from the Euphrates River varies within a range of about ± 25% of the measured discharges. Taking into account this assumption, we can prepare different operation scenarios.

The monthly actual evapotranspiration within the marsh was defined is given in **Figure 7**. The highest evapotranspiration was in June. Two factors govern the outflow required to flush out the accumulated salts within the marsh. The first is the total volume of the salt in the marsh water, and the second is how

much water can be supplied from the feeders, including the Al Khamissiya Canal. The maximum design capacity of the canal is 40 m^3/s which restricts the possible inflow. The amount of outflow from the west part of the Al-Hammar marsh positively affects the concentration of the TDS within the marsh. The more outflow, the more salt is flashed out.

The water budgeting was carried out, with the constraints of

- maintaining a constant area;
- the maximum design capacity of Al Khamissiya Canal is 40 m^3/s, and
- the discharge of the feeders of the marsh from the Euphrates River varies within a range of about ±25% of the measured discharges **Table 3** and

An example of the water budget calculation with different scenarios of water availability in the future **Table 4** shows the required inflow to maintain the maximum area of, e.g., 250 km^2 discharge of Al Khamissiya Canal is 15.6 m^3 /s, **Table 4** shows the monthly discharge can be released from the suggested outlet to reduce the salinity in the marsh, and the value of 3.6 m^3/s for June restricts a minimum outflow discharge.

With the same procedure can make different scenarios, e.g., under the condition that the feeders' discharges from the Euphrates River are 25% higher than the measured and a maximum inflow from Al Khamissiya Canal of 40 m^3/s, a maximum marsh area of 499 km^2 can be reached.

Table 3: Averages Sum of inflow to Al-Hammar marsh from Euphrates Rivers feeders from 2015-2017 m3 /s.

Month	Al Kurmashia	Um Nakhla	Right of Euphrates	Sum	Sum +25%	Sum -25%
Jan.	1.3	2.4	14.3	18.0	22.5	13.5
Feb.	1.6	2.7	10.6	14.9	18.6	11.2
Mar.	1.5	2.5	11.8	15.8	19.8	11.9
Apr.	1.6	2.7	16.6	20.9	26.1	15.7
May	1.2	2.5	11.5	15.2	19.0	11.4
Jun.	1.1	2.0	13.5	16.5	20.6	12.4
Jul.	1.7	2.3	14.8	18.8	23.5	14.1
Aug.	1.6	2.8	13.5	17.9	22.3	13.4
Sep.	1.8	3.3	14.0	19.0	23.8	14.3
Oct.	1.7	3.1	14.6	19.3	24.1	14.5
Nov.	1.2	2.1	6.7	10.1	12.6	7.5
Dec.	1.5	2.2	9.9	13.6	17.0	10.2
Averages	1.5	2.6	12.7	**16.7**	20.8	12.5

Table 4: The average release discharge from the suggested outlet to keep maintain the maximum area of 250 km^2 if the discharge of Al Khamissiya Canal is 15.6 m3 /s.

Month	Day	ET_a mm	ET_a m^3/s	Average monthly Rain fall mm	Rainfall m^3/s	Supplied Inflow from Euphrates River by Feeders m^3/s	Outflow m^3/s
Jan.	31	98	9.1	2.6	0.01	18.0	24.51
Feb.	28	155	16.0	10.9	0.04	14.9	14.59
Mar.	31	212	19.8	12.8	0.04	15.8	11.64
Apr.	30	267	25.7	4.3	0.01	20.9	10.90
May	31	285	26.6	0.2	0.00	15.2	4.20
Jun.	30	296	28.5	0.0	0.00	16.5	3.60
Jul.	31	288	26.9	0.0	0.00	18.8	7.50
Aug.	31	295	27.5	0.0	0.00	17.9	6.00
Sep.	30	257	24.8	0.0	0.00	19.0	9.80
Oct.	31	177	16.5	8.7	0.03	19.3	18.43
Nov.	30	115	11.1	5.6	0.02	10.1	14.62
Dec.	31	79	7.3	16.4	0.05	13.6	21.95
Averages		210	20	5.1	0.02	16.67	12.30

The calculation is made on monthly bases just to provide order on the magnitude, we can use actual evapotranspiration calculated in this study from satellite images and with develop two-dimensional hydrodynamic and water quality transport model with different scenarios and then analyses the results for the west part of the Al-Hammar marsh to know the optimum location of

the outlet and to simulate the distribution of the salt inside the marsh. The final decision about the area of the marsh and the target water quality parameters of the restoration is beyond the objectives of the present research; it has to be defined by the MoWR.

5 CONCLUSIONS AND SUGGESTIONS FOR THE FUTURE RESEARCH

5.1 Classification

In wetlands of arid and semi-arid regions, the land cover is very dynamic due to extreme driving factors, like high temperature, vapour deficit in the air, extreme rainfall events and floods on feeding rivers.

A classification approach was presented for monitoring marshlands by a hierarchical application of NDVI, NDMI, and NDWI indices calculated based on optical satellite images. The proposed automatic classification results in six land cover classes, namely, (1) open water, (2) dry area, (3) dense vegetation, (4) medium-density vegetation, (5) low-density vegetation, and (6) wet soil. The proposed method uses optical indices calculated from level-2 data, allowing the use of generic thresholds.

The results showed that the proposed methodology could efficiently classify marshlands and be used in different wetlands by changing the threshold for NDVI, NDMI, and NDWI.

The results prove that this approach is suitable for classifying marshlands with land cover types of water, dry soil, wet soil, and different densities of vegetation. Combining the long time series of Landsat images with new satellite data can also be recommended to provide more accurate classifications and increase revisiting times.

There is potential to develop our methodology to include other indices and other landcover groups.

5.2 Evapotranspiration

Our study evaluated two ET models, SEBS and SSEBop, and global ET products WaPOR and MOD 16, by comparing ET_0 from a metrological

station. SEBS and SSEBop models performed reasonably well in estimating ET_a.

Our comparison shows that the average ET_0 for 21 dates is 5.44 mm. On the basis of the results, the average ET_a values for SSEB, SSEBop, WaPOR and Mod16 are 5.03, 4.56, 2.60 and 4.38, respectively. The ET_a estimate showed that SEBS and SSEBop models effectively tracked ET_0 variation; during summer SSEBop shows higher ETa in open water and vegetation areas Compared with SEBS. The correlation between SEBS and ET_0 was the highest, and the SSEBop model needs to calibrate the *K* value. The WaPOR ETIa product showed the spatial and temporal variations, but the values were lower than SEBS, SSEBop and ET_0 during 2 years. This product has a problem with evaporation from the wet soil. Regarding the results, the WaPOR ET product is unreliable for estimating ET in this area, and MOD16 has an extremely coarse resolution. These products are unsuitable to use in small areas, and separating different ET from open water, vegetation and wet soil is difficult at this level of resolution. The higher ET_a for MOD16 from vegetation during summer and winter, MOD16 product recorded higher ET than the SEBS and SSEBop models value in some areas.

The results in estimating ET from the SEBS model are comparable with the SSEBop model, although SEBS is more complex and needs many input data. Comparing the data with ET_0 calculated from the data of the meteorological station showed that the R^2, RMSE and MAE values for the SEBS model are 0.89, 0.391 mm and 0.239, respectively, and are 0.881, 0.594 mm, and 0.449 for SSEBop, respectively. The SEBS model performed reasonably well in estimating ET_a with RMSE less than 0.5 mm day^{-1} **Tables 11** and **12**. Users should be careful in using the WaPOR and MOD16 products in marshland areas.

The accuracy of SEBS comes from using the data of the local metrological station. The wind speed (changing the ET process location due to water vapour displacement) and sunshine hour duration factors are important keys in estimating ET_a.

5.3 Calculated Water Balance

The results of the hydrological routing under the condition of the measured discharges showed that an inflow from Al Khamissiya Canal of 15.6 m^3/s and an annual average of the outflow of 33.6 m^3/s are required to maintain 250 km^2 of the west part of Al-Hammar marsh. Under the condition that the feeders' discharges from the Euphrates River are 25% higher than the measured and a maximum inflow from Al Khamissiya Canal of 40 m^3/s, a maximum marsh area of 499 km^2 can be reached. To maintain 250 km^2 of the marsh, when the discharges of the feeders from the Euphrates River are 25% higher than their measured values, the required flow from Al Khamissiya Canal is 11.5 m^3/s.

Moreover, the required inflow from the Al Khamissiya Canal to maintain a minimum area of 250 km^2 in the west part of the Al-Hammar marsh of when the discharges of the feeders from Euphrates River are 25% less than their measured values, is 19.7 m^3/s. Finally, in reducing the discharges of the feeders from the Euphrates River by 25%, the maximum area can reach up to 427 km^2 with a maximum discharge of Al Khamissiya Canal of 40 m^3/s.

6 NEW SCIENTIFIC RESULTS

A new scientific result of the dissertation can be summarised for the following five thesis:

1. I developed an optical indices-based hierarchical classification method for automatic land cover mapping to monitor the wetlands.
2. I proposed an optimum data processing method that locates the ET model as more sensitive in spatial and temporal.
3. I prepared and modified the actual ET curve that can be used in future water management studies.
4. I integrated and optimised the management data from different sources for feeding the regions with scarcity data.
5. I calculated the marsh's water balance to pinpoint the region that can be protected when water is abundant.

7 PUBLICATIONS

S. Al-Maliki, T. I. M. Ibrahim, G. Jakab, M. Masoudi, J. S. Makki, and Z. Vekerdy, "**An Approach for Monitoring and Classifying Marshlands Using Multispectral Remote Sensing Imagery in Arid and Semi-Arid Regions**," Water, vol. 14, no. 10, p. 1523, 2022. **I.F** (**3.530**). **Q1.**

T. I. M. Ibrahim, **S. Al-maliki**, and O. Salameh, "**Improving LST Downscaling Quality on Regional and Field-Scale by Parameterizing the DisTrad Method**," ISPRS International Journal of Geo-Information, vol. 11, no. 6, p. 327, 2022. **I.F.** (**3.099**) **Q1.**

Conference-proceedings

S. Al-maliki, Z. Vekerdy "**Assess the Status of The Marshlands with Regards to Inundation Area and Vegetation Cover Using Remote Sensing**", 21st Century Water Management in the Intersection of Sciences (publication), XXI. Századi vízgazdálkodás a tudományok metszéspontjában, Szent István Egyetem Agrár- és Gazdaságtudományi Kar, Scientific Conference in Szarvas, Hungary, (2019) pp. 336-342.

S. Al-maliki, Z. Vekerdy, "**Data Integration for Modelling of Environmental Impact of Using Brackish Water for Wetlands Restoration**", Advanced Training Course on Land Remote Sensing with the focus on Agriculture (Poster), Université Catholique de Louvain (Louvain-la-Neuve) – Belgium, 2019, http://landtraining2019.esa.int/page_posters.php.